Journal of Visualized Experiments

Human Fetal Blood Flow Quantification With Magnetic Resonance Imaging And Motion Compensation

--Manuscript Draft--

Article Type:	Invited Methods Collection - JoVE Produced Video
Manuscript Number:	JoVE61953R1
Full Title:	Human Fetal Blood Flow Quantification With Magnetic Resonance Imaging And Motion Compensation
Corresponding Author:	Datta Singh Goolaub University of Toronto Toronto, Ontario CANADA
Corresponding Author's Institution:	University of Toronto
Corresponding Author E-Mail:	datta.goolaub@sickkids.ca
Order of Authors:	Datta Singh Goolaub
	Davide Marini
	Mike Seed
	Christopher K. Macgowan
Additional Information:	
Question	**Response**
Please specify the section of the submitted manuscript.	Medicine
Please indicate whether this article will be Standard Access or Open Access.	Standard Access (US$2,400)
Please indicate the **city, state/province, and country** where this article will be **filmed**. Please do not use abbreviations.	Toronto, ON, Canada
Please confirm that you have read and agree to the terms and conditions of the author license agreement that applies below:	I agree to the Author License Agreement
Please provide any comments to the journal here.	

TITLE:

Human Fetal Blood Flow Quantification with Magnetic Resonance Imaging and Motion Compensation

AUTHORS AND AFFILIATIONS:

Datta Singh Goolaub[1,2], Davide Marini[3,4], Mike Seed[4,5], Christopher K. Macgowan[1,2]

[1]Department of Medical Biophysics, University of Toronto, Toronto, Ontario, Canada
[2]Division of Translational Medicine, The Hospital for Sick Children, Toronto, Ontario, Canada
[3]Labatt Family Heart Centre, The Hospital for Sick Children, Toronto, Ontario, Canada
[4]Department of Pediatrics, University of Toronto, Toronto, ON, Canada
[5]Division of Pediatric Cardiology, The Hospital for Sick Children, Toronto, ON, Canada

Corresponding Authors:
Datta Singh Goolaub (datta.goolaub@mail.utoronto.ca)
Christopher K. Macgowan (christopher.macgowan@sickkids.ca)

Email Addresses of Co-Authors:
Davide Marini (davide.marini@sickkids.ca)
Mike Seed (mike.seed@sickkids.ca)

KEYWORDS:

Fetal flow imaging with MRI, fetal phase contrast MRI

SUMMARY:

Here we present a protocol for measuring fetal blood flow rapidly with MRI and retrospectively performing motion correction and cardiac gating.

ABSTRACT:

Magnetic resonance imaging (MRI) is an important tool for the clinical assessment of cardiovascular morphology and heart function. It is also the recognized standard-of-care for blood flow quantification based on phase contrast MRI. While such measurement of blood flow has been possible in adults for decades, methods to extend this capability to fetal blood flow have only recently been developed.

Fetal blood flow quantification in major vessels is important for monitoring fetal pathologies such as congenital heart disease (CHD) and fetal growth restriction (FGR). CHD causes alterations in the cardiac structure and vasculature that change the course of blood in the fetus. In FGR, the path of blood flow is altered through the dilation of shunts such that the oxygenated blood supply to the brain is increased. Blood flow quantification enables assessment of the severity of the fetal pathology, which in turn allows for suitable *in utero* patient management and planning for postnatal care.

The primary challenges of applying phase contrast MRI to the human fetus include small blood vessel size, high fetal heart rate, potential MRI data corruption due to maternal respiration, unpredictable fetal movements, and lack of conventional cardiac gating methods to synchronize data acquisition. Here, we describe recent technical developments from our lab that have enabled the quantification of fetal blood flow using phase contrast MRI, including advances in accelerated imaging, motion compensation, and cardiac gating.

INTRODUCTION:

Comprehensive assessment of the fetal circulation is necessary for monitoring fetal pathologies such as fetal growth restriction (FGR) and congenital heart disease (CHD)[1–3]. In utero, patient management and planning for postnatal care depend on the severity of the fetal pathology[4–7]. Feasibility of fetal blood flow quantification with MRI and its applications in assessing fetal pathologies have recently been demonstrated[3,8,9]. The imaging method, however, faces challenges, such as increased imaging times to achieve high spatiotemporal resolution, lack of cardiac synchronization methods, and unpredictable fetal motion[10].

Fetal vasculature comprises small structures (~5 mm diameter for major blood vessels that comprise the descending aorta, ductus arteriosus, ascending aorta, main pulmonary artery, and superior vena cava[11–13]). To resolve these structures and to quantify flow, imaging at high spatial resolution is required. Moreover, the fetal heart rate is about twice that of an adult. A high temporal resolution is thus also required to resolve dynamic cardiac motion and blood flow across the fetal cardiac cycle. Conventional imaging at this high spatiotemporal resolution requires relatively long acquisition times. To address this issue, accelerated fetal MRI[14–16] has been introduced. Briefly, these acceleration techniques involve undersampling in the frequency domain during data acquisition and retrospective high-fidelity reconstruction using iterative techniques. One such approach is compressed sensing (CS) reconstruction, which allows reconstruction of images from heavily undersampled data when the reconstructed image is sparse in a known domain and undersampling artifacts are incoherent[17].

Motion in fetal imaging presents a major challenge. Motion corruption can arise from maternal respiratory motion, maternal bulk motion or gross fetal movement. Maternal respiration leads to periodic translations of the fetus, whereas fetal movements are more complex. Fetal movements can be classified as localized or gross[10,18]. Localized movements involve motion of only segments of the body. They typically last for about 10-14 s and their frequency increases with gestation (~90 per hour at term)[10]. These movements generally cause small corruptions and do not affect the imaging area of interest. However, gross fetal movements can lead to severe image corruption with through plane motion components. These movements are whole body movements mediated by the spine and last for 60-90 s.

To avoid artifacts from fetal motion, steps are first taken to minimize maternal motions. Pregnant women are made more relaxed using supportive pillows on the scanner bed and dressed in comfortable gowns and may have their partners present beside the scanner to reduce claustrophobia[19,20]. To mitigate effects of maternal respiratory motion, studies have performed

fetal MR exams under maternal breath-hold[21–23]. However, such acquisitions must be short (~15 s) given the reduced breath-hold tolerance of pregnant subjects. Recently, retrospective motion correction methods have been introduced for fetal MRI[14–16]. These methods track fetal motion using registration toolkits and correct for motion or discard uncorrectable portions of acquired data.

Finally, postnatal cardiac MR images are conventionally acquired using electrocardiogram (ECG) gating to synchronize data acquisition to the cardiac cycle. Without gating, cardiac motion and pulsatile flow from throughout the cardiac cycle are combined, producing artifacts. Unfortunately, the fetal ECG signal suffers from interference from the maternal ECG signal[24] and distortions from the magnetic field[25]. Hence, alternative non-invasive approaches to fetal cardiac gating have been proposed, including self-gating, metric optimized gating (MOG) and doppler ultrasound gating[21,26–28].

As described in the following sections, our MRI approach to quantify fetal blood flow leverages a novel gating method, MOG, developed in our laboratory and combined with motion correction and iterative reconstruction of accelerated MRI acquisitions. The approach is based on a pipeline in a previously published study[14] and is composed of the following five stages: (1) fetal blood flow acquisition, (2) real-time reconstructions, (3) motion correction, (4) cardiac gating, and (5) gated reconstructions.

PROTOCOL:

All MRI scans were performed with informed consent from volunteers as part of a study approved by our institutional research ethics board.

NOTE: The methods described below have been used on a 3T MRI system. The acquisition is performed using a radial phase contrast MRI sequence. This sequence was prepared by modifying the readout trajectory (to achieve a stellate pattern) of the manufacturer's Cartesian phase contrast MRI. The sequence and sample protocols are available upon request through our C^2P exchange platform. All reconstructions in this work were performed on a standard desktop computer with the following specifications: 32 GB memory, 3.40 GHz processor with 8 cores, and 2GB graphic card with 1024 compute unified device architecture (CUDA) cores. Image reconstruction was performed on MATLAB. Nonuniform fast Fourier transform (NUFFT)[29] was performed on the graphics processing unit (GPU). Motion correction parameters were calculated using elastix[30]. **Figure 1** depicts the protocol in a chronological order, tracking how the acquired velocity encodes (color coded in **Figure 1**) are processed with representative images at each stage of reconstruction. The reconstruction code is available at https://github.com/datta-g/Fetal_PC_MRI. While we provide the steps in the protocol here, most of these algorithm steps are automated in our pipeline.

1. Subject positioning and localizer exams

1.1. Assist the mother in positioning herself on the MRI table in her preferred comfortable position, usually supine or lateral decubitus positions, for the MRI exam.

1.2. Place the cardiac coil over the abdominal region of the mother.

1.3. Load the MRI table in the magnet bore and notify the mother that the scan is about to start.

1.4. Run a localizer exam to locate the fetal body (resolution: 0.9 x 0.9 x 10 mm^3, TE/TR: 5.0/15.0 ms, FOV: 450 x 450 mm^2, slices: 6).

1.5. Run a refined localizer exam to locate the fetal vasculature with the slice group centered on the fetal heart (resolution 1.1 x 1.1 x 6.0 mm^3, TE/TR: 2.69/1335.4 ms, FOV: 350 x 350 mm^2, slices: 10, orientation: axial to fetus).

1.6. Repeat the refined localizers with sagittal and coronal orientations for a clearer view of the fetal vessels.

1.7. Repeat the refined localizers in cases of gross fetal motion.

2. Acquisition of fetal blood flow data

2.1. Locate fetal vessels using the localizer exams. For example, the descending aorta is a long straight vessel near the spine in the sagittal planes. The ascending aorta and main pulmonary arteries can be identified as vessels leaving the left and right ventricles, respectively. The ductus arteriosus can be tracked as a downstream segment of the main pulmonary artery proximal to the descending aorta. The superior vena cava can be identified from axial planes near the base of the fetal heart as the vessel adjacent to the ascending aorta.

2.2. Prescribe a slice perpendicular to the axis of the fetal vessel of interest. Rotate and move the slice guideline on the MRI console computer such that it intersects the target vessel perpendicularly.

2.3. Set the scan parameters (acquisition type: radial phase contrast MRI, resolution: 1.3 x 1.3 x 5.0 mm^3, echo time (TE)/ repetition time (TR): 3.25/5.75 ms, field-of-view (FOV): 240 x 240 mm^2, slice: 1, velocity encoding: 100-150 cm/s depending on vessel of interest, velocity encoding direction: through plane, radial views: 1500 per encode, free breathing).

2.4. Run the scan and verify the prescription based on the initial time-averaged reconstruction performed and displayed on the MRI console computer. Repeat the localizer and phase contrast scans if the target vessel is absent or unidentifiable from the initial reconstruction. Acquired raw data is represented in the schematic in **Figure 1A** with the velocity compensated and through plane acquisitions color coded as red and blue, respectively.

2.5. Repeat the fetal blood data acquisition for each target blood vessel.

NOTE: The acquired raw data (format: DAT files) must be transferred for offline reconstruction. For example, on Siemens scanners, this can be performed by running 'twix'. The acquired raw data is right clicked from the list acquisitions and "copy total raid file" is chosen.

3. Motion correction of fetal measurements

3.1. Reconstruct real-time series (temporal resolution: 370 ms, radial views: 64) from the acquired data using CS with 15 iterations of a conjugate gradient descent optimization exploiting spatial total variation (STV, weight: 0.008) and temporal total variation (TTV, weight: 0.08) regularization as represented by the schematic in **Figure 1B**.

3.2. Select a region of interest (ROI) encompassing the vessel of interest from this first real-time reconstruction using a graphic user interface developed in MATLAB. In this step, the user must draw a contour that encloses the fetal anatomy, such as the target great vessels or the fetal heart.

3.3. Perform rigid-body motion tracking with elastix[30] (based on normalized mutual information with empirically optimized parameters: 4 pyramid levels, 300 iterations and translational transforms).

3.4. Reject tracked real-time frames that share low mutual information (MI) with all other frames (whereby MI is less than 1.5x the interquartile range from the mean MI). These frames are deemed to be represented through plane motion or gross fetal motion.

3.5. Use the MRI data corresponding to the longest series of continuous real-time frames (without gaps) from the remaining frames as the quiescent period used for further reconstruction.

3.6. Interpolate translational motion correction parameters from the temporal resolution of the real-time series (370 ms) to the TR of the quiescent acquisition (5.75 ms).

3.7. Apply interpolated parameters to the defined quiescent period of the MRI data by modulating the phase as in:

$$s'(k_x, k_y) = s(k_x, k_y)e^{-2\pi j(k_y\Delta_y + k_x\Delta_x)}$$

where s' is the motion corrected data, k_x and k_y are the coordinates in k-space, s is the acquired uncorrected data, Δ_x and Δ_y are the tracked displacements in space, and j represents $\sqrt{-1}$.

NOTE: All numerical values of regularization coefficients in this work were optimized in earlier experiments. This was accomplished using a brute-force grid search to find the regularization

coefficients that minimized the error between reconstructions of a highly sampled fetal reference dataset and retrospectively undersampled cases from the same dataset.

4. Solving for fetal heart rate

4.1. Reconstruct a second real-time image series at a higher temporal resolution (temporal resolution: 46 ms, radial views: 8) using the acquired data using CS, again with 15 iterations of a conjugate gradient descent optimization with STV (weight: 0.008) and TTV (weight: 0.08) regularization as represented by the schematic in Figure 1C.

4.2. Re-select an ROI encompassing the fetal vessel of interest.

4.3. Run multiparameter MOG on the real-time series to derive the time-dependent fetal heart rate.

4.4. Bin motion corrected MRI data into 15 cardiac phases using the derived heart rate waveform. In this step, the temporal boundaries of the cardiac phases are computed using the heart rate from the previous step. For instance, the boundaries for the i^{th} phase in the k^{th} heartbeat are given by:

$$\left(HR(k) + (i-1)\frac{HR(k+1) - HR(k)}{15}\right) \quad \& \quad \left(HR(k) + i\frac{HR(k+1) - HR(k)}{15}\right)$$

where $HR(k)$ is the time at which the k^{th} heartbeat occurs. The timestamp of the n^{th} radial acquisition is given by (n x TR). Data with timestamps falling within the boundaries of a cardiac phase are assigned to that phase.

NOTE: MOG is a gating technique[26] that comprises iterative binning of the acquired data based on a multi-parameter fetal heart rate model to create CINE images that optimize an image metric over a region of interest.

5. Reconstruction of fetal CINEs

5.1. Reconstruct fetal flow CINEs using the binned motion corrected MRI data and CS with 10 iterations of a conjugate gradient descent optimization with STV (weight: 0.025) and TTV (weight: 0.01) regularization. Two CINEs are produced at this step: one for the flow compensated acquisition, C_{FC} and one with the flow encoded data, C_{FE}, as represented in the schematic in **Figure 1D**.

5.2. Compute the velocity image given by the phase of the elementwise product of C_{FE} and the complex conjugate of C_{FC}.

5.3. Apply background phase correction[31] to correct for eddy current effects. Briefly, in this automatic step, a plane is fitted to the phase of static fetal and maternal tissues. The correction is performed by subtracting the plane from the velocity sensitive phase computed in 4.2.

5.4. Write reconstructed data into DICOM files.

5.5. Load DICOMs into flow analysis software, such as Segment v2.2[32].

5.6. Draw an ROI encompassing the lumen of the blood vessel of interest using the anatomical and velocity sensitive images.

5.7. Propagate the ROI to all cardiac phases and correct for changes in the vessel's diameter.

5.8. Record flow measurements.

REPRESENTATIVE RESULTS:

In general, phase MRI examinations of flow target six major fetal vessels: the descending aorta, ascending aorta, main pulmonary artery, ductus arteriosus, superior vena cava, and umbilical vein. These vessels are of interest to the clinician as they are often implicated in CHD and FGR, influencing the distribution of blood throughout the fetus[9]. A typical scan duration with the radial phase contrast MRI is 17 s per vessel such that the scans are short while also allowing time for enough data acquisition for CINE reconstruction. The total acquisition time, including localizers and phase contrast MRI, for the representative results was 3 min. In this study, representative results are presented using flow acquisition data from the descending aorta in two human fetuses: Fetus 1 and Fetus 2 with gestational ages (week + days) of 35+4 and 37+3, respectively.

As in **Figure 1**, initial real-time reconstructions (temporal resolution: 370 ms) performed for motion tracking took 45 s per reconstructed slice. Translation motion tracking took 2 min for each slice. The extracted motion parameters for Fetus 1 (**Figure 2 A1**, maximum displacement: 1.6 mm) and Fetus 2 (**Figure 2 A2**, maximum displacement: 1.3 mm) depict the motion of the descending aorta over the duration of the scan. The shared mutual information of each real-time frame with all other co-registered frames are shown in **Figure 2 B1** (Fetus 1) and **Figure 2 B2** (Fetus 2). In these cases, all frames shared mutual information above the cut off criteria, so no data was rejected. The second real-time reconstructions (temporal resolution: 46 ms), used to derive cardiac gating information, took 10 min for each slice. MOG derived the fetal heartbeat (RR) intervals using a multiparameter model, as shown in **Figure 2 C1** (Fetus 1, RR interval: 521 ± 20 ms) and **Figure 2 C2** (Fetus 2, RR interval: 457 ± 9 ms).

Final CINE reconstructions using the retrospectively motion-corrected and gated data took 3 min per slice. The anatomical and velocity reconstructions for Fetus 1 and Fetus 2 at peak systole are shown in **Figure 3**. Reconstructions with motion correction show vessels with sharper walls. Without motion correction, the descending aorta is blurrier and less conspicuous. The measured flow curves from each fetus (**Figure 4**) show higher peak and mean flows in the reconstructions

without motion correction ([peak mean]: Fetus 1 [25.2 9.8] ml/s, Fetus 2 [34.6 10.3] ml/s]) than in those with motion correction ([peak mean]: Fetus 1 [23.5 9.2] ml/s, Fetus 2 [28.7 9.7] ml/s]).

FIGURE AND TABLE LEGENDS:

Figure 1: Pipeline to reconstruct fetal phase contrast MRI data. (A) Step 1: Golden-angle radial phase contrast MRI data (color coded as: flow compensation = red & through plane encode = blue). The alternating colors depict that the flow-compensated and through-plane encoded acquisitions occur at the same spatial frequencies. (B) Step 2: Temporal windows of 370 ms for real-time reconstruction using CS with sparsity constraints (STV and TTV). Motion correction and data rejection are performed. (C) Step 3: Temporal windows of 46 ms are created for real-time reconstruction with CS (with STV and TTV sparsity constraints) for MOG. (D) Step 4: The data is binned into cardiac phases (CP), and CS is used to create a fetal flow CINE, with sparsity constraints (STV and TTV). Representative reconstructions from each CS step are shown in the Reconstructions column. Reconstructions for steps 3 and 4 are shown for a time point corresponding to peak systole. Scale bars in the top left corner of the anatomical images denote 10 mm in the image. The time specifications, in seconds, highlighted in grey represent the durations of the corresponding steps. STV: spatial total variation, TTV: temporal total variation, CS: compressed sensing, MOG: metric optimized gating, CINE: gated dynamic reconstruction.

Figure 2: Representative displacement and heart rate curves. A1 and A2 depict retrospectively tracked displacement curve for the scans in Fetus 1 and Fetus 2, respectively. B1 and B2 show the sum of the mutual information of a given frame with all other frames for Fetus 1 and Fetus 2, respectively. The red dotted lines represent 1.5x interquartile range below which data is rejected. C1 and C2 depict the RR intervals derived with MOG in Fetus 1 and Fetus 2, respectively. RR interval: time between consecutive heartbeats, MOG: metric optimized gating.

Figure 3: Representative velocity sensitive CINE reconstructions at peak systole. Each quadrant depicts the anatomical and velocity reconstructions. The top row shows the CINE with motion correction in Fetus 1 and Fetus 2, respectively. The bottom row shows the CINE without motion correction in Fetus 1 and Fetus 2, respectively. The red and blue arrows depict the descending aorta. Scale bars in the top left corner of the anatomical images denote 10 mm.

Figure 4: Representative flow curves in the fetal descending aorta. The solid and dashed data lines depict the flow curves obtained from CINE reconstructions with and without motion correction, respectively, in Fetus 1 (left) and Fetus 2 (right).

DISCUSSION:

This method enables the non-invasive measurement of blood flow in human fetal great vessels and allows for retrospective motion correction and cardiac gating by making use of iterative reconstruction techniques. Fetal blood flow quantification has been performed with MRI in the past[1, 3, 8, 9]. These studies had a prospective approach to mitigate motion corruption whereby scans would be repeated if gross fetal motion was visually identified from an initial reconstruction on the scanner. The current protocol improves on this by retrospectively rejecting data corrupted by gross fetal motion and further corrects for in-plane displacements arising from subtle fetal

movements or maternal respiratory motion.

This protocol makes use of a multiparameter model for MOG whereby the RR interval for each fetal heartbeat is calculated. Using a low parameter heart rate model (such as 2 parameters) is generally acceptable for short scans since the healthy fetal heart rate has a low variability[33]. However, low parameter models become problematic for longer scans or in cases of pathologies such as arrythmia. A multiparameter model in MOG can track these changing RR intervals, providing more accurate flows.

The current protocol allows for some modifications. First, third party software used in this study for motion tracking and flow analysis can be replaced by other available software packages. Second, the number of iterations in the conjugate gradient descent algorithms for CS can be increased. In this study, the number of iterations in each step was set at a value beyond which there were minimal improvements based on prior reconstructions. In this work, only third trimester pregnancies were scanned. In earlier pregnancies, the fetus is smaller and there may be more room for motion. However, since quiescent periods in the scan are identified retrospectively for CINE reconstructions, this protocol should be successful for flow imaging at these earlier ages. An increase in the resolution of the scans may be required to cater to smaller vessel diameters at lower gestational age. For this protocol, the reconstruction times reported in **Figure 1** and the Results are heavily dependent on the computational power available. For example, with better GPUs and more powerful processors, reconstruction times can be significantly reduced.

The protocol has certain limitations. First, the quality of the CINE reconstruction depends on the amount of data rejected in the motion correction step. With increasing episodes of gross fetal movements during a scan, more data is rejected. Consequently, the resulting signal-to-noise ratio (SNR) in the CINE reconstructions will decrease. Low SNR increases the uncertainty in the velocity images[34] and the resulting flow quantification. Performance will therefore improve with greater fetal quiescence. Second, the method depends on the definition of ROIs for motion correction and MOG. In the current implementation, this step is performed manually. We have found that the reconstruction is stable to small differences in ROI position but this process results in wait times between the data acquisition and CINE reconstructions (since there are two ROI placement steps between the three iterative reconstruction steps). This becomes more cumbersome when there is a large number of slices acquired. In future implementations of the protocol, ROI placement will be automated.

Currently, we are using the presented protocol in research studies with approval from the local ethics board. The protocol can also be used in cases in which motion is a potential problem during an MRI exam, such as in neonates or uncooperative subjects. Future directions of the method involve investigating spiral trajectories[35,36], which provide more efficient sampling and a possibility for exploring real-time fetal flow.

ACKNOWLEDGMENTS:
None.

DISCLOSURES:

None.

REFERENCES:

1. Zhu, M.Y. et al. The hemodynamics of late-onset intrauterine growth restriction by MRI. *American Journal of Obstetrics and Gynecology*. **214** (3), 367.e1-367.e17 (2016).
2. Zhu, M.Y., Jaeggi, E., Roy, C.W., Macgowan, C.K., Seed, M. Reduced combined ventricular output and increased oxygen extraction fraction in a fetus with complete heart block demonstrated by MRI. *HeartRhythm Case Reports*. **2** (2), 164–168 (2016).
3. Sun, L. et al. Reduced Fetal Cerebral Oxygen Consumption is Associated With Smaller Brain Size in Fetuses With Congenital Heart Disease. *Circulation*. **131** (15), 1313–1323 (2015).
4. Freud, L.R. et al. Fetal aortic valvuloplasty for evolving hypoplastic left heart syndrome: postnatal outcomes of the first 100 patients. *Circulation*. **130** (8), 638–645 (2014).
5. Peleg, D., Kennedy, C.M., Hunter, S.K. Intrauterine growth restriction: identification and management. *American Family Physician*. **58** (2), 453–460, 466–467 (1998).
6. Krishna, U., Bhalerao, S. Placental Insufficiency and Fetal Growth Restriction. *Journal of Obstetrics and Gynaecology of India*. **61** (5), 505–511 (2011).
7. Seravalli, V., Miller, J.L., Block-Abraham, D., Baschat, A.A. Ductus venosus Doppler in the assessment of fetal cardiovascular health: an updated practical approach. *Acta Obstetricia et Gynecologica Scandinavica*. **95** (6), 635–644 (2016).
8. Seed, M. et al. Feasibility of quantification of the distribution of blood flow in the normal human fetal circulation using CMR: a cross-sectional study. *Journal of Cardiovascular Magnetic Resonance*. **14** (1), 79 (2012).
9. Prsa, M. et al. Reference ranges of blood flow in the major vessels of the normal human fetal circulation at term by phase-contrast magnetic resonance imaging. *Circulation. Cardiovascular Imaging*. **7** (4), 663–670 (2014).
10. Piontelli, A. *Development of Normal Fetal Movements: The Last 15 Weeks of Gestation*. Springer-Verlag. Mailand. (2015).
11. Cartier, M. et al. The normal diameter of the fetal aorta and pulmonary artery: echocardiographic evaluation in utero. *American Journal of Roentgenology*. **149** (5), 1003–1007 (1987).
12. Ruano, R., de Fátima Yukie Maeda, M., Niigaki, J.I., Zugaib, M. Pulmonary artery diameters in healthy fetuses from 19 to 40 weeks' gestation. *Journal of Ultrasound in Medicine*. **26** (3), 309–316 (2007).
13. Nowak, D., Kozłowska, H., Żurada, A., Gielecki, J. Diameter of the ductus arteriosus as a predictor of patent ductus arteriosus (PDA). *Central European Journal of Medicine*. **6** (4), 418–424 (2011).
14. Goolaub, D.S. et al. Multidimensional fetal flow imaging with cardiovascular magnetic resonance: a feasibility study. *Journal of Cardiovascular Magnetic Resonance*. **20** (1), 77 (2018).
15. Roy, C.W., Seed, M., Kingdom, J.C., Macgowan, C.K. Motion compensated cine CMR of the fetal heart using radial undersampling and compressed sensing. *Journal of Cardiovascular Magnetic Resonance*. **19** (1), 29 (2017).

16. Amerom, J.F.P. van et a*l.* Fetal cardiac cine imaging using highly accelerated dynamic MRI with retrospective motion correction and outlier rejection. *Magnetic Resonance in Medicine*. **79** (1), 327–338 (2018).
17. Lustig, M., Donoho, D., Pauly, J.M. Sparse MRI: The application of compressed sensing for rapid MR imaging. *Magnetic Resonance in Medicine*. **58** (6), 1182–1195 (2007).
18. Edwards, D.D., Edwards, J.S. Fetal movement: development and time course. *Science (New York, N.Y.)*. **169** (3940), 95–97 (1970).
19. Malamateniou, C. *et al.* Motion-Compensation Techniques in Neonatal and Fetal MR Imaging. *American Journal of Neuroradiology*. **34** (6), 1124–1136 (2013).
20. Rutherford, M. et al*.* MR imaging methods for assessing fetal brain development. *Developmental Neurobiology*. **68** (6), 700–711 (2008).
21. Haris, K. et al*.* Self-gated fetal cardiac MRI with tiny golden angle iGRASP: A feasibility study: Self-Gated Fetal Cardiac MRI with iGRASP. *Journal of Magnetic Resonance Imaging*. **46** (1), 207–217 (2017).
22. Glenn, O.A. MR imaging of the fetal brain. *Pediatric Radiology*. **40** (1), 68–81 (2010).
23. Rodríguez-Soto, A.E., et al. MRI Quantification of Human Fetal O2 Delivery Rate in the Second and Third Trimesters of Pregnancy. *Magnetic Resonance in Medicine*. **80** (3), 1148–1157 (2018).
24. Sameni, R., Clifford, G.D. A Review of Fetal ECG Signal Processing; Issues and Promising Directions. *The Open Pacing, Electrophysiology & Therapy Journal*. **3**, 4–20 (2010).
25. Millis, R. *Advances in Electrocardiograms: Methods and Analysis*. BoD – Books on Demand. (2012).
26. Jansz, M.S. et al*.* Metric optimized gating for fetal cardiac MRI. *Magnetic Resonance in Medicine*. **64** (5), 1304–1314 (2010).
27. Yamamura, J. et al*.* Cardiac MRI of the fetal heart using a novel triggering method: initial results in an animal model. *Journal of Magnetic Resonance Imaging: JMRI*. **35** (5), 1071–1076 (2012).
28. Larson, A.C., et al. Self-gated cardiac cine MRI. *Magnetic Resonance in Medicine*. **51** (1), 93–102 (2004).
29. Knoll, F., Schwarzl, A., Diwoky, C., Sodickson, D.K. gpuNUFFT-An open source GPU library for 3D regridding with direct Matlab interface. *Proceedings of the 22nd Annual Meeting of ISMRM* (2014).
30. Klein, S., Staring, M., Murphy, K., Viergever, M.A., Pluim, J.P.W. elastix: a toolbox for intensity-based medical image registration. *IEEE Transactions on Medical Imaging*. **29** (1), 196–205 (2010).
31. Walker, P.G., et al. Semiautomated method for noise reduction and background phase error correction in MR phase velocity data. *Journal of Magnetic Resonance Imaging*. **3** (3), 521–530 (1993).
32. Heiberg, E., et al. Design and validation of Segment - freely available software for cardiovascular image analysis. *BMC Medical Imaging*. **10** (1), 1 (2010).
33. Inder, T.E., Volpe, J.J. Chapter 17 - Intrauterine, Intrapartum Assessments in the Term Infant. *Volpe's Neurology of the Newborn (Sixth Edition)*. 458-483.e8 (2018).
34. Pelc, N.J., Herfkens, R.J., Shimakawa, A., Enzmann, D.R. Phase contrast cine magnetic resonance imaging. *Magnetic Resonance Quarterly*. **7** (4), 229–254 (1991).
35. Steeden, J.A., Atkinson, D., Hansen, M.S., Taylor, A.M., Muthurangu, V. Rapid flow assessment of congenital heart disease with high-spatiotemporal-resolution gated spiral phase-

contrast MR imaging. *Radiology*. **260** (1), 79–87 (2011).
36. Kowalik, G.T., Knight, D., Steeden, J.A., Muthurangu, V. Perturbed spiral real-time phase-contrast MR with compressive sensing reconstruction for assessment of flow in children. *Magnetic Resonance in Medicine*. **83** (6), 2077–2091 (2020).

Figure 1

Click here to access/download;Figure;Figure 1.tif

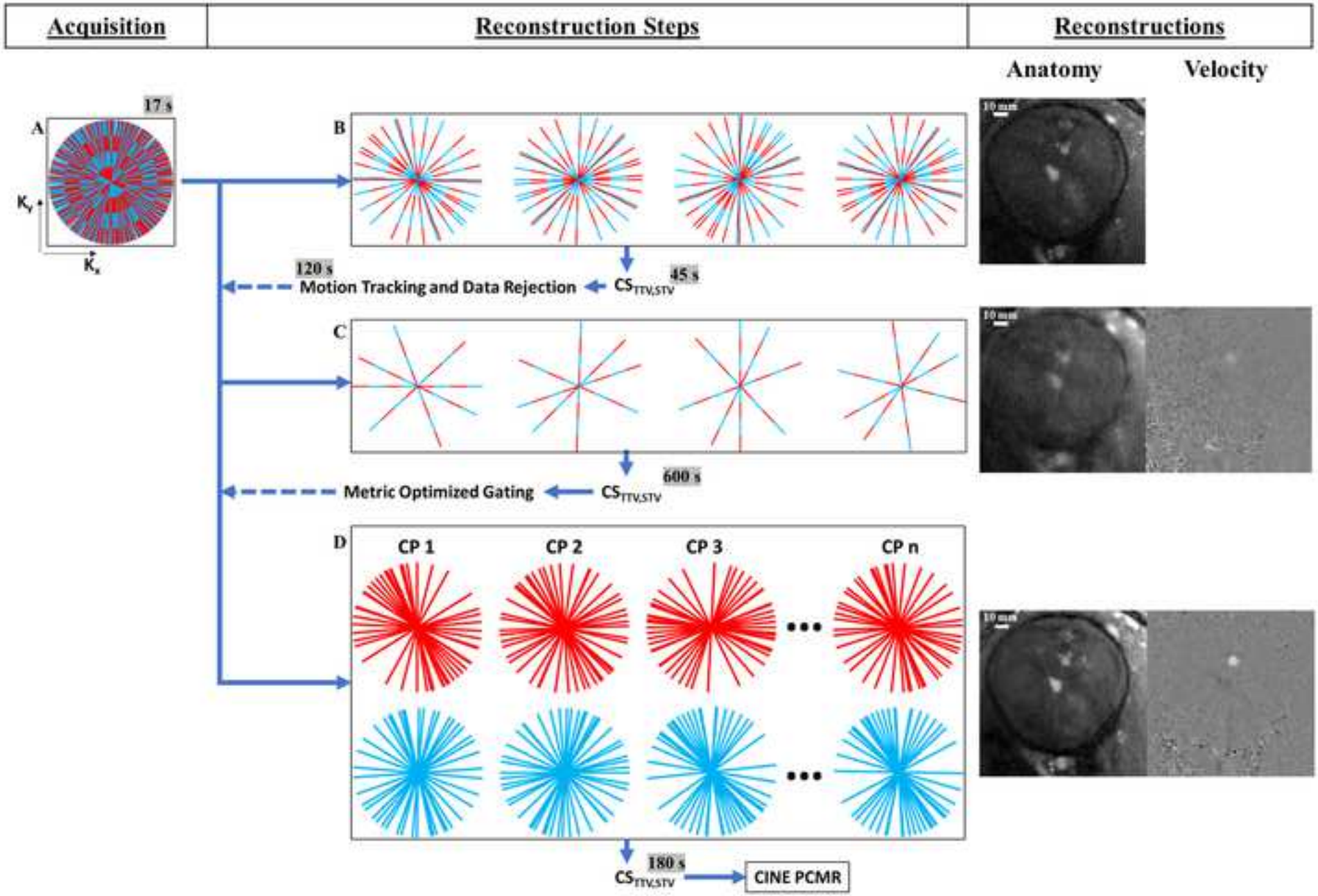

Figure 2

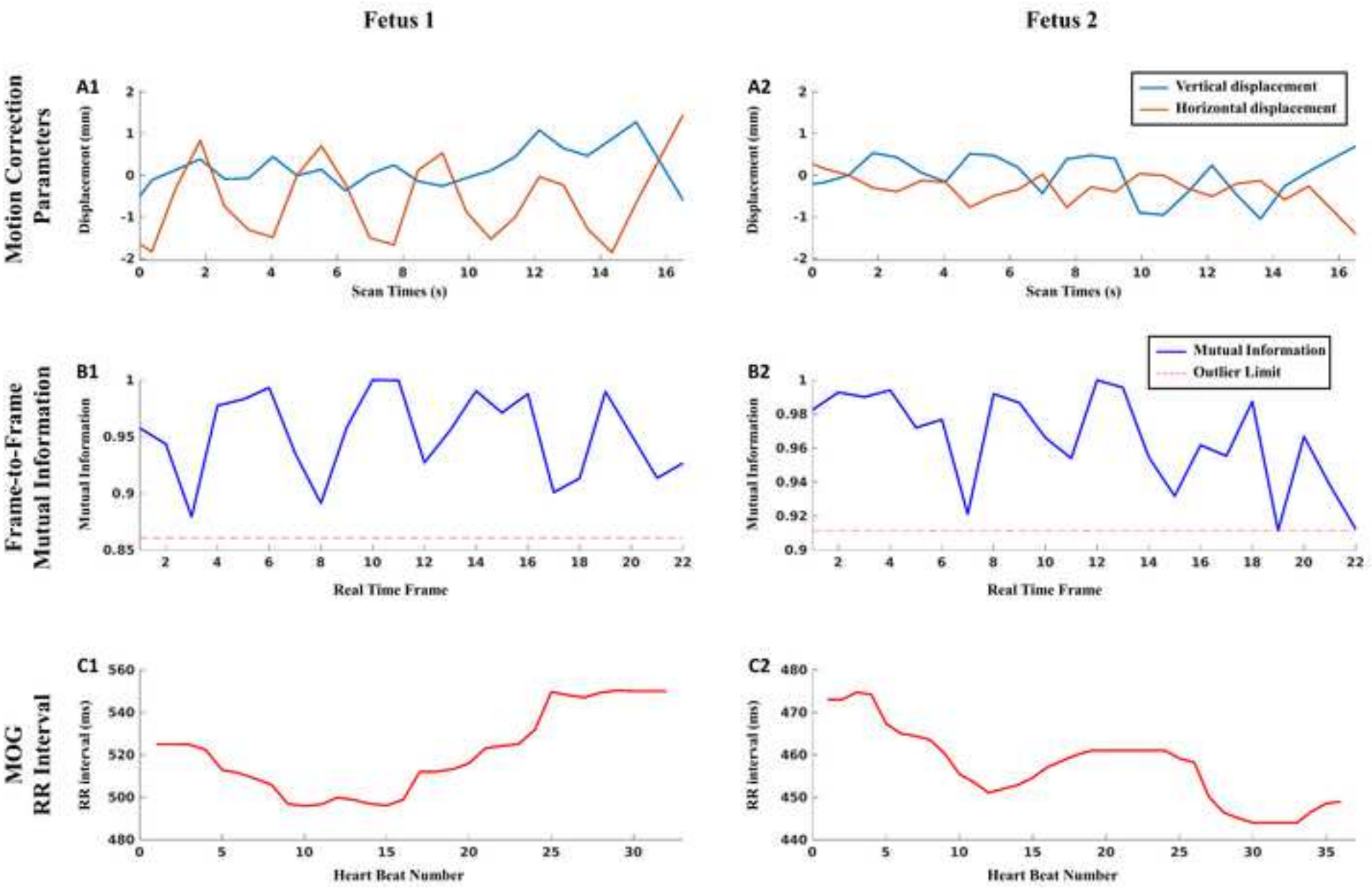

Figure 3

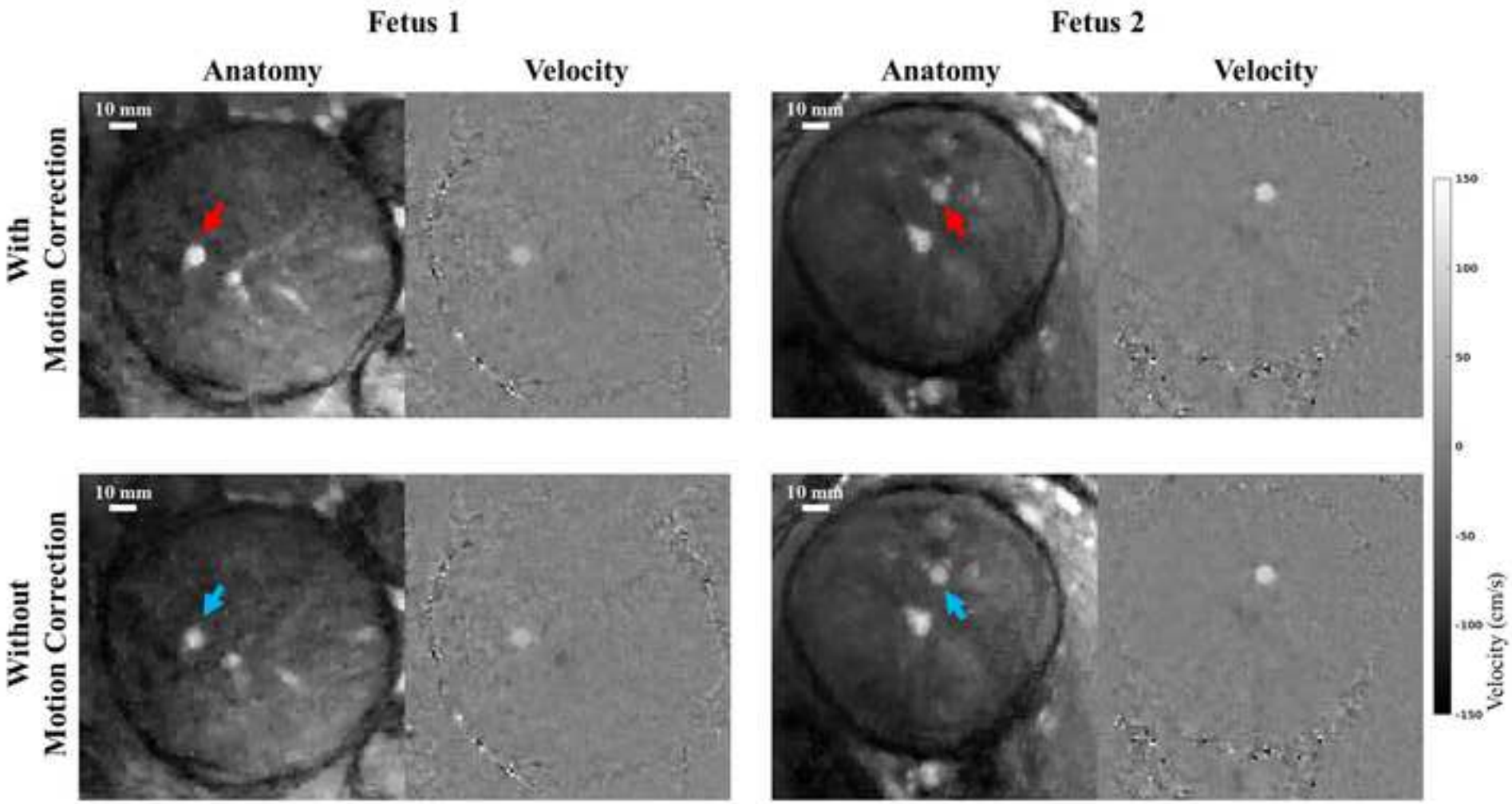

Figure 4

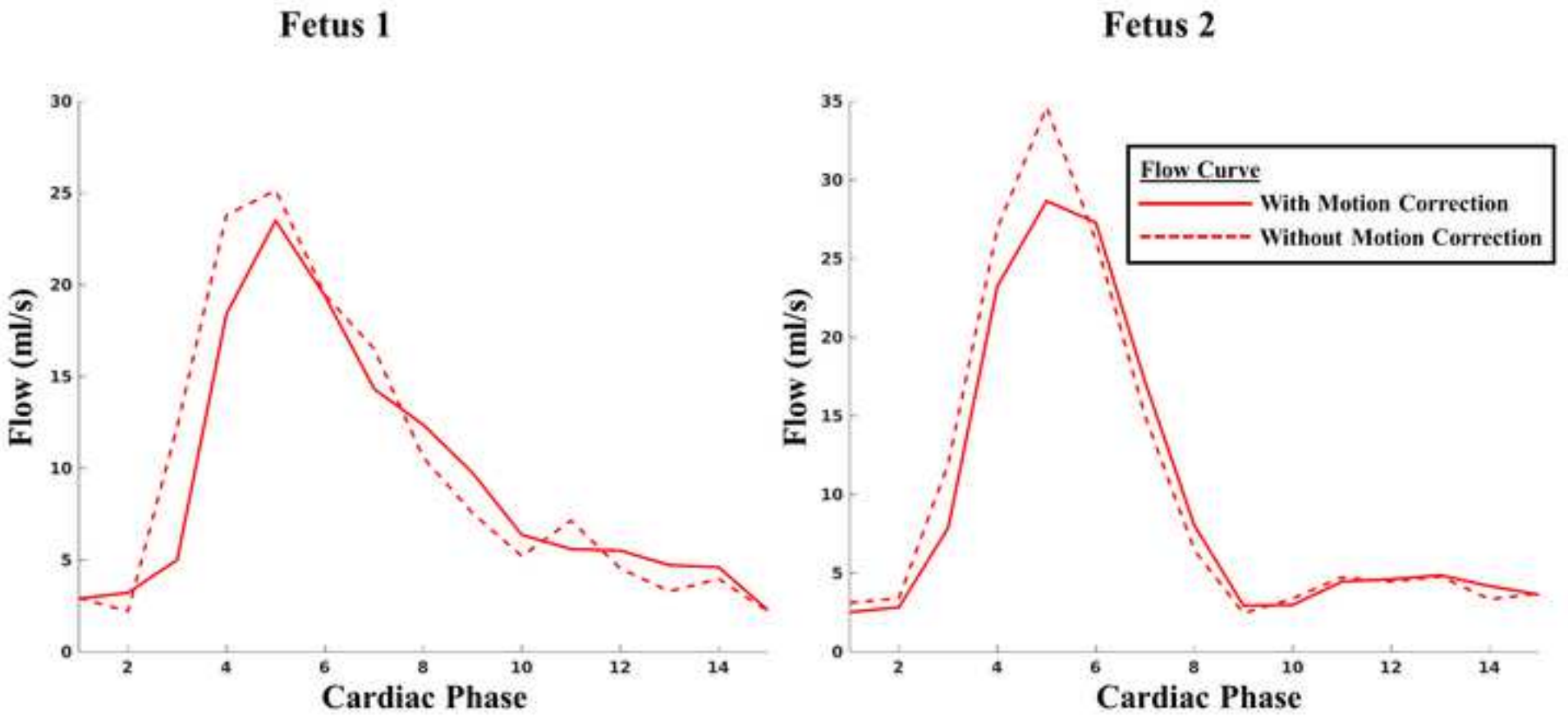

Name of Material/ Equipment	Company	Catalog Number
elastix	Image Sciences Institute, University Medical Center Utrecht	
Geforce GTX 960	Nvidia	04G-P4-3967-KR
gpuNUFFT	CAI²R	
MAGNETOM Prisma	Siemens	10849583
MATLAB	MathWorks	
Radial Phase Contrast MRI sequence		
Segment	Medvisio	
VENGEANCE	Corsair	LPX DDR4-2666

Comments/Description

Image registration software

Non-uniform fast Fourier transform

Trajectory modification of manufacturer's Cartesian Phase Contrast sequence
Data analysis

We thank the editors and reviewers for their constructive feedback. We have addressed all comments to produce a more rigorous manuscript, as detailed below in our point-by-point response:

Response to editor

Thank you for your feedback. Major editor comments were related to reorganization of the text and adding specifics to the steps in the protocol. We have addressed all requests and provide a high-level summary of these changes below. Responses in the annotated document are labelled E# corresponding to these requests. Responses to all remarks can be followed in the document with tracked changes by searching for 'E#' where # is the identifier of the review from the Editor's feedback.

Comment 3: The editor pointed out that title must be more concise. (see E3)

Response: We have changed the title of our manuscript to emphasize the use of MRI and the motion correction aspects of the work.

Comment 6: The editor pointed out that the summary must be in full sentences. (see E6)

Response: We have rephrased our summary into a full sentence.

Comment 9, 10, 11, 12: The editor pointed out that additional details were required in the protocol. (see E9. E10, E11, E12)

Response: We have updated our protocol by adding more details in various steps and the first paragraphs of the Protocol section.

Comment 13: The editor pointed out that all figures must be referenced in the text and to comment on the significance of reconstruction times. (see E13)

Response: There was a typo in the final paragraph of the Results section where Figure 3 was referenced as Figure 2. We have corrected this now. Moreover, we have listed reconstruction times in Figure 1 and added comments in the Discussion section stating how these reconstruction times depend on computational architecture.

Comment 14: The editor requested that scale bars be specified in the caption of figures. (see E14)

Response: We have now added a sentence in the captions of Figure 1 and Figure 3 stating what the scale bars represent.

Comment 15: The editor pointed out that some references had to be corrected to the correct style. (see E15)

Response: Done.

Response to reviewer #1

The reviewer had some minor edits for the document. We have labelled our response for these reviews as 1.X# where # is the comment number under each heading and X is I for Introduction, P for Protocol, R for Representative Results and D for Discussion as per the heading used by the reviewer.

Comment Introduction 1: The reviewer pointed out that maternal gross motion is also a concern. (See 1.I1)

Response: We agree with the reviewer and maternal gross motion is a concern in fetal imaging. We have listed it as an additional source of corruption in the Introduction.

Comment Introduction 2: The reviewer requested that we stated more clearly what we were imaging. (See 1.I2)

Response: We have added the term 'flow' to the ambiguous sentence to make it clear that we are looking at flow measurement.

Comment Introduction 3: The reviewer requested that we specify major fetal blood vessels. (See 1.I3)

Response: We have now listed the major fetal blood vessels along with the references in the Introduction.

Comment Introduction 4: The reviewer requested a reference for fetal motion. (See 1.I4)

Response: We have now referenced Piontelli's work on fetal motion in late gestation.

Comment Protocol 1: The reviewer asked whether the sequence is available. (See 1.P1)

Response: We have now added a sentence stating that the sequence is available for download from the Siemens C^2P platform with the reconstruction tool being available on our GitHub page soon.

Comment Protocol 2: The reviewer asked clarification on subject positioning. (See 1.P2)

Response: We have now added a new section in the protocol which details the position of the subject on the scanner bed and the localizers used.

Comment Protocol 3 and 4: The reviewer asked whether all steps are repeated for each vessel and if there are quality checks performed on the measurements. (See 1.P3 and 1.P4)

Response: We have a step specifying that the localizers are repeated only if gross fetal motion occurred. A review of the time-averaged image reconstructed on the scanner shows whether there was gross fetal motion. Hence, if there is no visible fetal motion during the scan (see step 2.4), the same localizers can be used to prescribe all flow measurements in all vessels.

Comment Representative Results 1: The reviewer asked to comment on total acquisition time. (See 1.R1)

Response: We have now added a sentence stating the total acquisition time for the localizers and the phase contrast MRI used for the Representative Results in the manuscript.

Comment Discussion 1: The reviewer asked to comment on the possibility of using this approach at lower gestational age. (See 1.D1)

Response: We state that in this work, we only scanned third trimester pregnancies. We can comment that in earlier pregnancy, the fetus is smaller and there may be more room for motion. However, since quiescent periods in the scan are identified retrospectively for CINE reconstructions here, the approach should be successful in flow imaging.

Comment Discussion 2: The reviewer asked to comment on the possibility of using this approach as part of a clinical exam. (See 1.D2)

Response: We have added a sentence that we are using this approach for REB approved research studies. For clinical use, the protocol needs to be formally approved by the Department of Pediatrics as a Quality Improvement policy.

Response to reviewer #2

Reviewer #2 had comments regarding the clarifications on Figure 1 and specifics on background correction in the Protocol. Moreover, the reviewer had 4 comments (2, 3, 4, and 9) which conveyed a similar message; the crux of these comments was that the manuscript lacked validation and seems different from usual manuscripts the reviewer has seen. In line with the philosophy of JoVE, the work presented here is for a Methods collection which describes the detailed protocol of our previously validated experiments. Therefore, the manuscript focuses on the different steps in our protocol (with the highlighted lines denoting video recording as per the guidelines of the journal) and representative results that a reader would obtain if the steps presented in the protocol were followed. References to previous publications of their validation are provided. Additional details on the aim of this manuscript can be found at: https://www.jove.com/methods-collections/about and https://www.jove.com/methods-collections/376/techniques-for-studying-blood-flow. We have labelled our responses as 2.# for the major concerns and 2.#m for the minor concerns.

Comment 6: The reviewer asked for clarifications on the values of the parameters chosen for registration and compressed sensing. (See 2.6)

Response: We have added details in the protocol on how these values were found from empirical testing and grid searches in our prior experiments. Once these values were found, they are not changed for subsequent reconstructions.

Comment 7: The reviewer asked to clarify the color codes in Figure 1. (See 2.7)

Response: We have now added clarifications throughout the manuscript and in the legend of Figure 1 regarding the blue and red colors used. We believe that the text is less ambiguous now. The alternating colors along the same spoke meant that the 2 encodes occurred at the

same spatial frequencies. By separating them in the Figure 1D, we mean that they are processed to provide two CINEs.

Comment 8: The reviewer asked to clarify on the background phase correction. (See 2.8)

Response: We have added details that static maternal and fetal tissues are used for the correction. We have also briefly described the algorithm in the referenced Walker et al. paper.

Minor comments can be tracked as 2.#m in the manuscript. Briefly, these changes included removing some unnecessary text, clarifications on fetal blood vessels and rationale for acquisition time. We chose 17 s to make the scans short for clinical exams while also allowing for enough data to be available for compressed sensing reconstructions.